Heliyon 9 (2023) e17223

Contents lists available at ScienceDirect

Heliyon

journal homepage: www.cell.com/heliyon

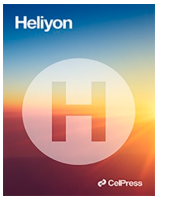

Integrated bioinformatics analysis reveals the function and prognostic value of OSBPL3 in hepatocellular carcinoma

Yuanshuai Su [1], Chen Xue [1], Xinyu Gu, Yu Sun, Renfang Zhang, Lanjuan Li [*]

State Key Laboratory for Diagnosis and Treatment of Infectious Diseases, National Clinical Research Center for Infectious Diseases, National Medical Center for Infectious Diseases, Collaborative Innovation Center for Diagnosis and Treatment of Infectious Diseases, The First Affiliated Hospital, Zhejiang University School of Medicine, 79 Qingchun Rd., Hangzhou, 310003, China

ARTICLE INFO

Keywords:
OSBPL3
Hepatocellular carcinoma
Prognosis
Immune infiltration
Hub gene

ABSTRACT

Background: Liver hepatocellular carcinoma (LIHC), a variety of highly-aggressive malignancy, has been the major cause of cancer-related mortality. Recent studies have shown that oxysterol-binding protein-like 3 (OSBPL3) plays a crucial role in human cancers. Nevertheless, the specific functional roles and potential clinical values of OSBPL3 in LIHC are not completely known.
Methods: Multiple web portals and publicly available tools were used in this study. Comprehensive expression files of OSBPL3 in pan-cancers and the relationship between OSBPL3 expression and clinical traits of patients with LIHC were investigated using TCGA database through UALCAN platform. TIMER database was used to investigate the effect of OSBPL3 on the tumor immune infiltration status in LIHC. Moreover, LinkedOmics, STRING databases, and Gene Ontology analysis were utilized to select OSBPL3-related differentially expressed genes (DEGs) and construct a protein–protein interaction (PPI) network.
Results: Upregulated OSBPL3 was observed in LIHC tumor tissues compared with that in normal controls, especially in patients with higher grades and more advanced stages. Furthermore, overexpressed OSBPL3 was closely associated with poor clinical outcomes of patients with LIHC. Six hub genes were selected from the PPI network, which were significantly increased in LIHC and closely associated with poor prognosis. Pathway enrichment showed that OSBPL3-related DEGs were primarily enriched in protein binding, mitotic cytokinesis, inorganic anion transport, and I-kappaB kinase/NF-kappaB signaling processes.
Conclusions: OSBPL3 exerts critical functions in hepatocarcinogenesis and it could serve as an available biomarker and effective treatment target for LIHC.

1. Introduction

Primary liver cancer was one of the most highly-aggressive malignancies worldwide. Cancer statistics reported that liver cancer has been the sixth most frequently diagnosed cancer and the third major cause of tumor-related mortalities globally, with 9,05,677 newly diagnosed cases and 9,30,180 deaths in 2020 [1,2]. Liver hepatocellular carcinoma (LIHC), accounting for approximately 80% of the total cases, is the most common histological subtype of liver cancer. It is characterized by high malignancy, poor therapeutic response, and unfavorable clinical outcomes [3,4]. Unfortunately, owing to the lack of early effective monitoring and inadequate intervention,

* Corresponding author.
E-mail address: ljli@zju.edu.cn (L. Li).
[1] Yuanshuai Su and Chen Xue contributed equally.

https://doi.org/10.1016/j.heliyon.2023.e17223
Received 20 February 2023; Received in revised form 8 June 2023; Accepted 10 June 2023
Available online 12 June 2023

the majority of patients with LIHC are at advanced stages when diagnosed, which results in poor clinical outcomes and higher mortality rates (1-year survival rate <20%) [5], thereby heavily burdening global health. Despite plentiful studies on the pathogenesis of LIHC, it remains necessary to explore novel biomarkers or promising therapeutic targets and perform a comprehensive analysis on the underlying mechanisms of hepatocarcinogenesis.

Oxysterol-binding protein-like 3 (OSBPL3) is a novel member of the oxysterol-binding protein (OSBP) family [6]. As an intracellular lipid receptor and transporter [7], which regulates lipid metabolism and vesicular transport under physiological conditions, and also participates in cell signaling transduction and cytoskeleton structure regulation [8–10]. Recently, studies have shown that OSBPs were significantly dysregulated at the mRNA or protein levels in diverse cancers [11,12]. The high expression level of OSBPL3 was positively associated with poor clinical outcomes and high malignancy of patients with colorectal cancer (CRC) [13,14]. Therefore, the mRNA levels of OSBPL3 can be a promising diagnostic biomarker to better stratify patients with CRC. Aberrant OSBPL3 functions can affect many pathophysiological processes, such as cell cycle progression and cell migration, thereby modulating the oncogenesis of diverse human cancers. Nevertheless, the biological roles of OSBPL3 in LIHC and its underlying interaction networks are largely unexplored.

In this study, we comprehensively investigated the comprehensive expression signature of OSBPL3 in pan-cancers and revealed its relationship with the clinicopathological features and tumor immune infiltration of patients with LIHC, thereby highlighting the prognostic value of OSBPL3. Furthermore, to discover the specific functional roles of OSBPL3 in LIHC, we screened differentially expressed gene (DEG) for OSBPL3 and constructed a protein–protein interaction (PPI) network, thereby providing novel insights into the initiation and progression of LIHC.

2. Method and materials

2.1. Clinical datasets and survival analysis

The informative data of OSBPL3 expression files in pan-cancers and the comprehensive clinical records related to LIHC were retrieved from TCGA database (https://cancer.gov/tcga) through the UALCAN platform (http://ualcan.path.uab.edu), a web-portal resource for analyzing clinical datasets [15]. Based on the obtained clinical informative data, patients with LIHC were divided into different subgroups and the correlation between OSBPL3 expression and clinical features of patients with LIHC was further determined.

To verified the clinical value of OSBPL3 as a prognostic indicator for LIHC, we used the Kaplan-Meier Plotter (https://kmplot.com/analysis/), an interactive web-portal resource, to perform univariate Cox regression for survival analysis [16]. We divided LIHC cohorts into two subgroups based on the expression of OSBPL3. The Kaplan-Meier prognosis curves with hazard ratios and log-rank *P*-values were plotted, which included overall survival (OS), disease-specific survival (DSS), progression-free survival (PFS), and relapse-free survival (RFS).

2.2. OSBPL3-related DEGs screening

To visualize and analyze the complex LHIC genomic data, we used the cBioportal database (https://www.cbioportal.org/) to screen co-expressed genes for OSBPL3, and the correlation coefficients were determined by Spearman's analysis [17]. For further verification, the LinkedOmics database (http://linkedomics.org/) was used to determine the OSBPL3-related DEGs as described in a previous study [18], for which general data was displayed in the Volcano maps (−log10 P value). Through the Z-Score analysis, heatmaps showed the top 15 positive and 15 negative OSBPL3-related genes, respectively.

PPI network construction and identified hub genes.

The SRING database (http://string-db.org/) was used to transform identified or predicted associations between the genes and proteins into biological understanding through physical interactions and functional network analysis [19]. In this study, the STRING database was used to construct a PPI network based on the top 100 related DEGs for OSBPL3. Then, we used the Cytoscape software as described previously [20], to visualize and analyze large-volume networks with appearance and characteristics from the STRING database. Finally, six hub genes were selected from the network, and their clinical values in indicating prognosis for LIHC were further investigated using the UALCAN database and the Kaplan-Meier curve.

2.3. Functional gene enrichment analysis

Gene ontology (GO) functional enrichment analysis based on detected 100 DEGs was performed to determine the related signaling pathways, assigning functional significance to OSBPL3 from three major domains of biological process, molecular function, and cellular component. A set of analysis tools for functional annotation and integration, which included the DAVID database (https://david.ncifcrf.gov/) and online bioinformatics resources (http://www.bioinformatics.com.cn/), were used to visualize and analyze the functional enrichment analysis results [21].

2.4. Immune infiltration status evaluation

To determine the interaction between OSBPL3 expression and LIHC immune status, we used the TIMER database (https://cistrome.shinyapps.io/timer/), which is an integrated web server to analyze tumor immune infiltration as described previously [22]. Spearman

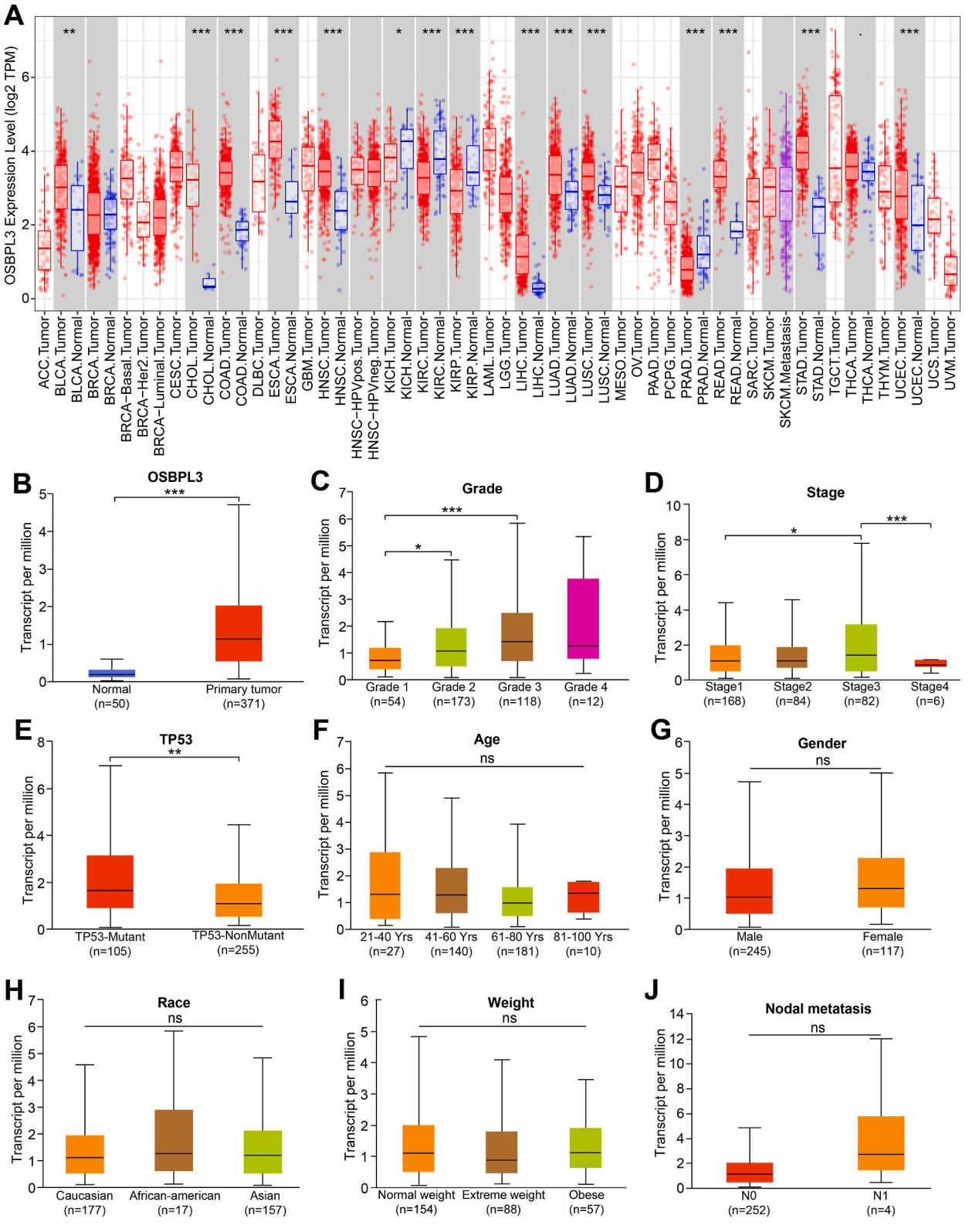

(caption on next page)

Fig. 1. Comprehensive analysis of the transcription levels of OSBPL3 in pan-cancers and its correlation with the clinicopathological features of patients with LIHC. (A). Transcription levels of OSBPL3 across pan-cancers. (B) Critically upregulated OSBPL3 in LIHC tissues compared with the normal control. (C–J) Transcription levels of OSBPL3 in diverse clinical characteristic-based groups (grade, stage, TP53 mutation, age, gender, race, weight and nodal metastasis). Abbreviations: OSBPL3, oxysterol-binding protein-like 3; LIHC, liver hepatocellular carcinoma.

analysis was performed to estimate the relationship between OSBPL3 and immune purity and immune-cell infiltration in LIHC.

2.5. Statistical analysis

Wilcoxon and *t*-tests were performed to determine the differences in OSBPL3 expression across subgroups of different variables. The relationship between OSBPL3 expression and multiple variables, such as immune-cell infiltration, was evaluated by the Spearman correlation co-efficiency test. *P*-values <0.05 were considered statistically significant. R program (v 4.0.3) and forest plot were used to visualize the informative data and build graphs.

3. Results

3.1. Overexpressed OSBPL3 in LIHC and its relationship with clinical characteristics

The transcription levels of OSBPL3 were dysregulated in most types of cancers compared with that in the normal controls (Fig. 1A). Particularly, the transcription level of OSBPL3 was significantly increased in LIHC tumor tissue (n = 371) compared with that in the normal control (n = 50, $P < 0.001$, Fig. 1B). In further to determine the roles of OSBPL3 in clinical LIHC progress, we categorized the comprehensive clinical datasets into different subgroups based on the diverse clinicopathological characteristic of patients with LIHC. Our findings showed that OSBPL3 gradually increased with the progression of tumor grade (grade 3 vs. grade 1, $P < 0.001$; grade 2 vs. grade 1, $P < 0.05$; Fig. 1C). Intriguingly, in patients with more advanced tumor stages, a significantly higher expression of OSBPL3 (stage 3 vs. stage 1, $P < 0.05$, Fig. 1D) was found, which indicated the oncogenic roles of OSBPL3 in LIHC progression. Furthermore, the expression of OSBPL3 in patients with mutant TP53 gene was critically upregulated than those without TP53 gene mutation ($P < 0.01$, Fig. 1E). Whereas, there was no significant correlation between OSBPL3 expression and gender, age, lymph node metastasis, and the race of patients with LIHC (Fig. 1F–J).

3.2. Evaluation of the prognostic value of OSBPL3 in LIHC

We next employed Kaplan-Meier survival analysis to investigate the prognostic value of OSBPL3 in LIHC. Based on OSBPL3 expression, we divided patients of LIHC cohorts into highly and lowly OSBPL3-expressed subgroups. Our findings showed that in the highly OSBPL3-expressed subgroup, patients with LIHC had a poorer prognosis than the other subgroup. Kaplan-Meier survival curves showed that patients with LIHC with highly-expressed OSBPL3 had shorter survival times including OS [HR = 1.72 (1.2–2.45), log-rank $P = 0.0026$], RFS [HR = 1.92 (1.23–2.99), log-rank $P = 0.0033$], PFS [HR = 0.78 (0.58–1.07), log-rank $P = 0.12$], and DSS [HR = 0.62 (0.44–0.87), log-rank $P = 0.0054$] (Fig. 2A–D). Taken together, overexpressed OSBPL3 was critically correlated with poor clinical outcomes of patients with LIHC, indicating its clinical value as a prognostic biomarker.

3.3. OSBPPL3 mutations and co-expressed genes screening

In LIHC, the somatic mutation frequency of OSBPL3 in LIHC was 1.7%, and the observed mutations were all missense mutations

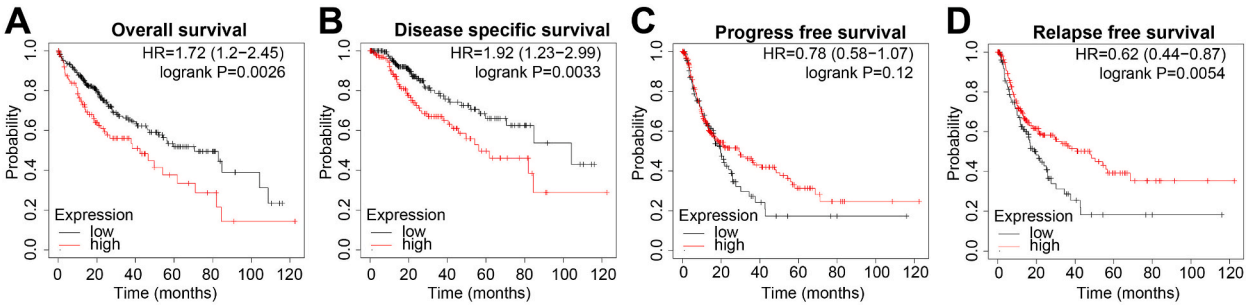

Fig. 2. Kaplan-Meier survival curves of patients with liver LIHC based on OSBPL3 expression. (A–D) Patients with LIHC in the highly-expressed OSBPL3 subgroup have a poor prognosis. Kaplan-Meier survival curves show OS [HR = 1.72 (1.2–2.45), log-rank p = 0.0026), DSS [HR = 1.92 (1.23–2.99), log-rank p = 0.0033], PFS [HR = 0.78 (0.58–1.07), log-rank p = 0.12], and RFS [HR = 0.62 (0.44–0.87), log-rank p = 0.0054). Abbreviations: LIHC, liver hepatocellular carcinoma; OSBPL3, oxysterol-binding protein-like 3; HR, hazard ratio; OS, overall survival; DSS, disease-free survival; PFS, progression-free survival; RFS, relapse free survival.

(Fig. 3A). Furthermore, the effect of putative copy-number variations, including shallow deletion, diploid, gain, and amplification on OSBPL3 mRNA expression, are shown in Fig. 3B. Then, we screened the co-expressed genes for OSBPL3 using the cBioportal database. The following top six most significantly co-expressed genes were selected: DCXR (Spearman coefficient: −0.60), FAM225B (Spearman coefficient: 0.61), GRHPR (Spearman coefficient: −0.62), NFE2L3 (Spearman coefficient: 0.62), PDE7A (Spearman coefficient: 0.60), and TRAF5 (Spearman coefficient: 0.61) (Fig. 3C–H).

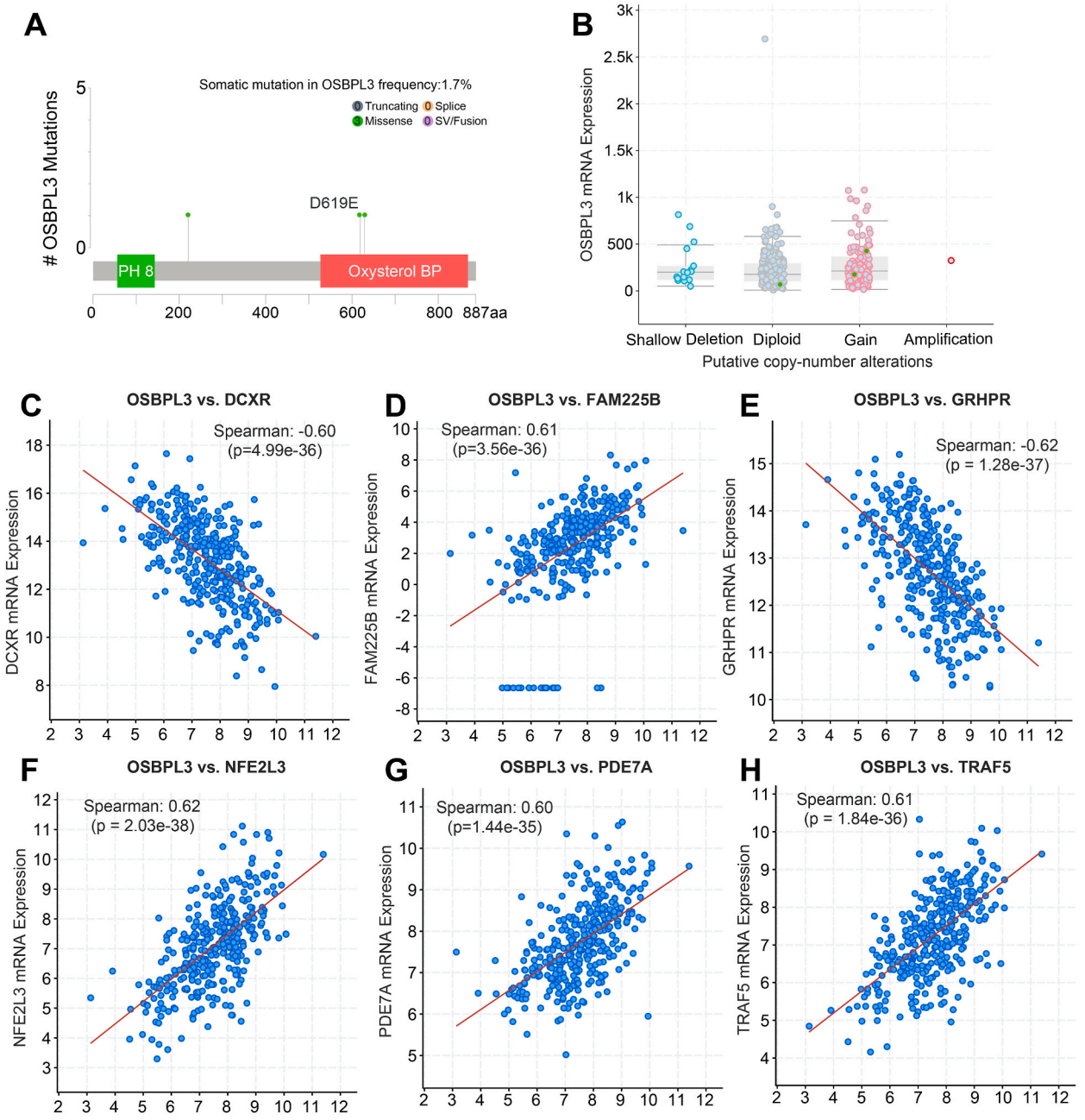

Fig. 3. Somatic mutations and co-expressed genes for OSBPL3. (A) The somatic mutation frequency of OSBPL3 in LIHC was 1.7%. (B) Effect of putative copy-number alterations on OSBPL3 mRNA expression. (C–H) The top six critically co-expressed genes for OSBPL3: *DCXR* (Spearman coefficient: −0.60), *FAM225B* (Spearman coefficient: 0.61), *GRHPR* (Spearman coefficient: −0.62), *NFE2L3* (Spearman coefficient: 0.62), *PDE7A* (Spearman coefficient: 0.60), and *TRAF5* (Spearman coefficient: 0.61). Abbreviations: OSBPL3, oxysterol-binding protein-like 3; LIHC, liver hepatocellular carcinoma.

3.4. Correlation between OSBPL3 and LIHC immune-cell infiltration

Furthermore, we explored the effect of overexpressed OSBPL3 on tumor immune status using the TIMER database and determined the correlation between OSBPL3 expression and immune purity and immune-cell infiltrating levels in LIHC. The correlation coefficient was calculated based on Partial Spearman's rho values. We found that OSBPL3 expression was slightly correlated with LIHC immune purity (cor = −0.187, p = $4.57e^{-04}$). Furthermore, positive correlations were observed between OSBL3 expression and the infiltration levels of six types of immune cells, which included B cells (cor = 0.378, p = $3.70e^{-13}$), $CD8^+$ T cells (cor = 0.313, p = $3.44e^{-09}$), $CD4^+$ T cells (cor = 0.543, p = $9.58e^{-28}$), macrophages (cor = 0.553, p = $1.00e^{-28}$), neutrophils (cor = 0.451, p = $1.91e^{-18}$), and dendritic cells (cor = 0.432, p = $6.58e^{-17}$) (Fig. 4A). We further investigated the effect of somatic copy-number variations for OSBPL3 on the infiltration levels of various immune cells. As shown in Fig. 4B, the OSBPL3 copy-number variation was critically correlated with the infiltration levels of B cells, $CD4^+$ T cells, neutrophils, and dendritic cells ($P < 0.05$ for all). Collectively, these results revealed a close relationship between OSBPL3 and LIHC tumor immune status, providing new viewpoints for LIHC immunotherapy.

3.5. OSBPL3-related DEGs and PPI network construction

We investigated the biological roles and the integrated interaction network of OSBPL3 in LIHC using the LinkedOmics database and detected OSBPL3-related DEGs comprehensively. A total of 13,311 genes ($P < 0.05$) were identified, and the OSBPL3 association results are shown in a volcano plot (Fig. 5A). The top 15 negatively and 15 positively correlated DEGs are presented in heatmaps, respectively (Fig. 5B–C). Based on the top 100 related genes, we further constructed an integrated PPI network using the STRING database to broaden our understanding of the OSBPL3 core regulatory network (Fig. 5D). Moreover, six hub genes, namely *CEP55*, *KIF23*, *DEPDC1B*, *ANLN*, *IQGAP1*, and *ECT2*, were identified from the interaction network visualized using the Cytoscape software (Fig. 5E). The comprehensive landscape of the biological roles of OSBPL3 in interaction networks might provide novel perspectives to study hepatocarcinogenesis.

3.6. Expression and prognostic value evaluation of the hub genes in LIHC

Next, the prognostic values of the six hub genes mentioned above were further explored in the LIHC cohort. Intriguingly, the transcriptional levels of all hub genes were critically higher in the LIHC tissue samples than in the normal controls ($P < 0.001$, Fig. 6A–F). In addition, Kaplan-Meier survival analysis was employed to detect the effect of upregulated hub genes on the survival of patients with LIHC. The results showed that patients with LIHC with highly-expressed hub genes had a poorer prognosis than those

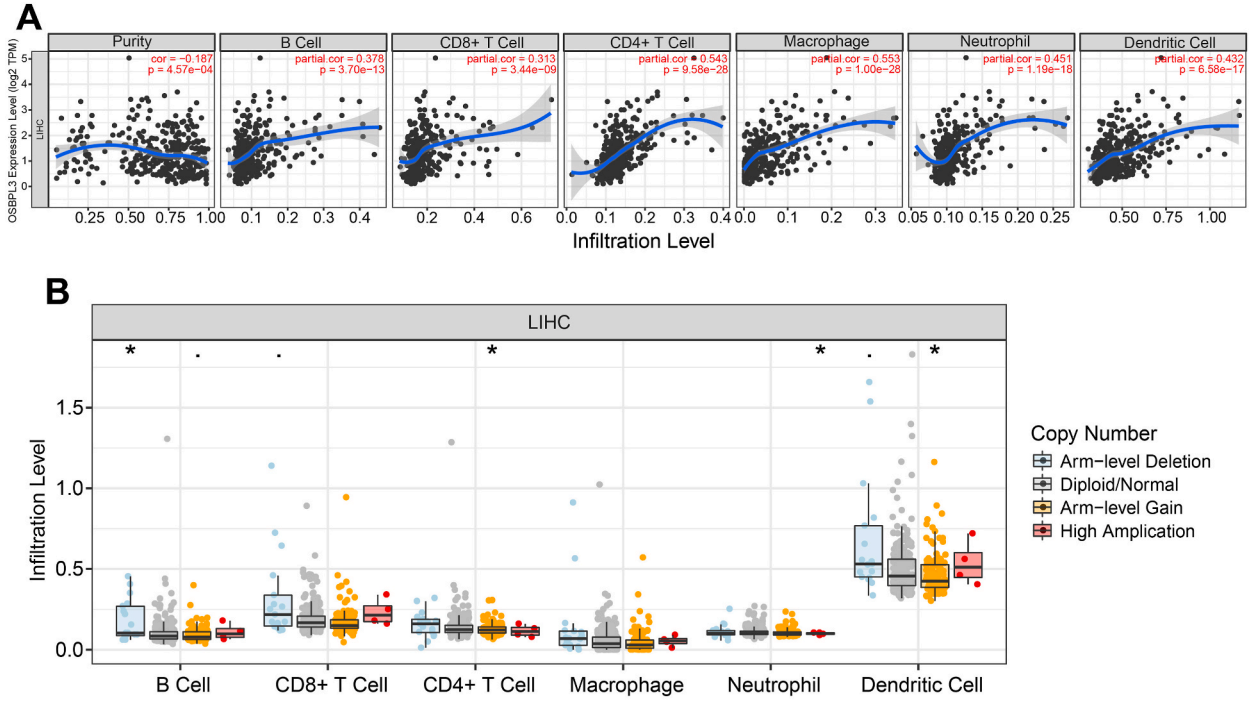

Fig. 4. Relationship between OSBPL3 expression and LIHC immune infiltration status. (A) Correlation analysis between OSBPL3 expression and immune purity and six types of immune cells, namely B-cell, CD8+-T cell, CD4+-T cell, macrophage, neutrophil, and dendritic-cell infiltration. (B) OSBPL3 copy-number variation affects the infiltration levels of immune cells in LIHC. Abbreviations: OSBPL3, oxysterol-binding protein-like 3; LIHC, liver hepatocellular carcinoma.

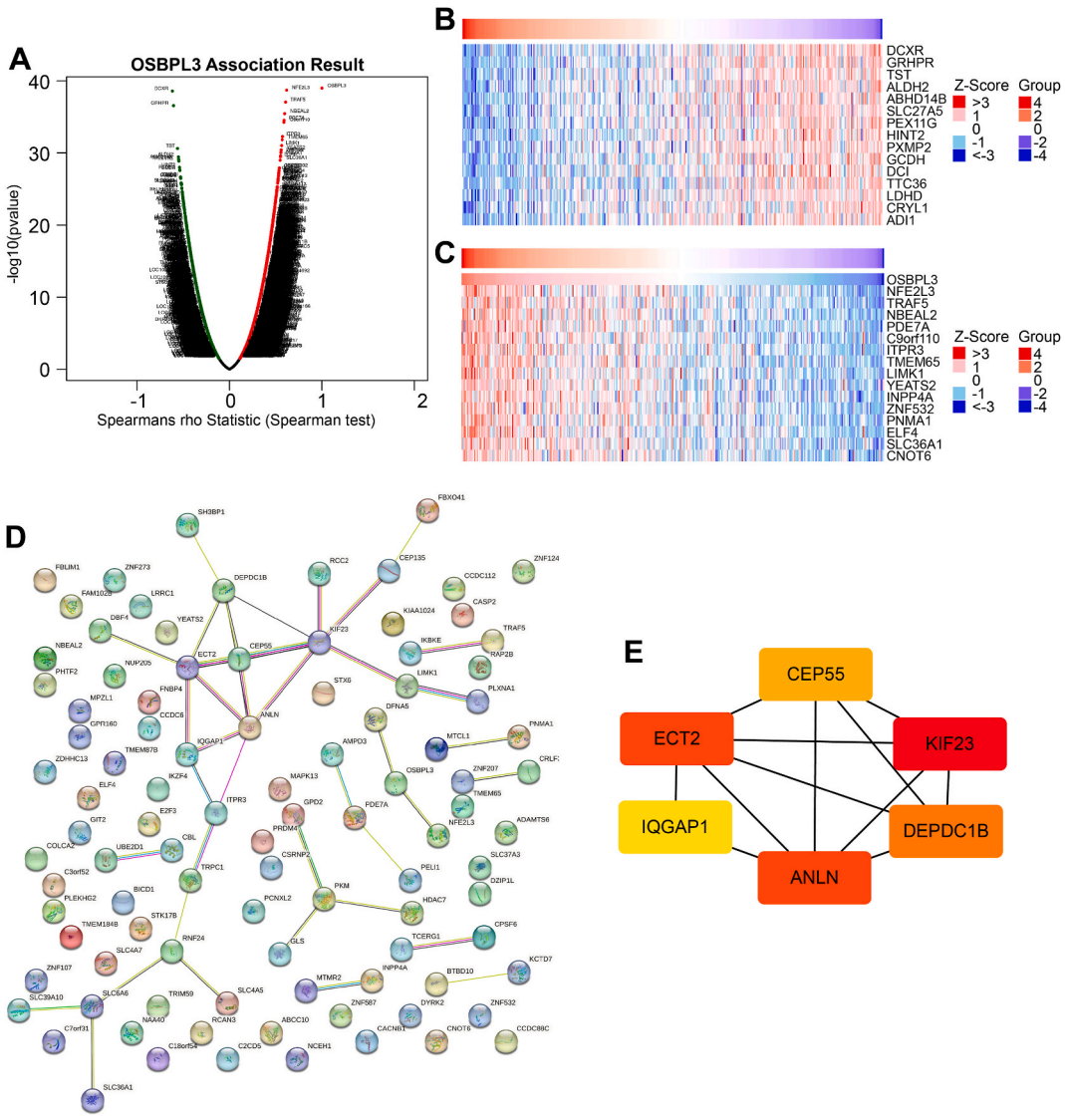

Fig. 5. DEGs for OSBPL3 screening and the PPI network. (A) Volcano plots show the comprehensive results of OSBPL3-associated genes. (B–C) Heatmaps display the top 15 negatively associated and 15 positively associated OSBPL3-related DEGs, respectively. (D) Construction of the PPI network based on the top 100 related DEGs. (E) Six hub genes were selected from the network: *CEP55*, *KIF23*, *DEPDC1B*, *ANLN*, *IQGAP1*, and *ECT2*. Abbreviations: DEGs, differentially expressed genes; PPI, protein-protein interaction; OSBPL3, oxysterol-binding protein-like 3.

with low-expressed hub genes (Fig. 6G–L). Therefore, our results implied that the detected hub genes might be high-risk factors for LIHC.

3.7. Functional gene enrichment analysis based on OSBPL3-related DEGs

OSBPL3, an intracellular lipid receptor, exerts diverse effects on various biological pathways. The GO enrichment analysis for functional pathway annotation showed that OSBL3-related DEGs were mainly enriched in the biological and functional pathways, including protein binding, mitotic cytokinesis, inorganic anion transport, and I-kappa B kinase/NF-kappa B signaling. The DEGs were enriched in various CCs, such as the cytosol, mid-body, and nucleus. The bar diagrams of the top 10 significantly enriched pathways of three categories of BP, MF, and CC are shown in Fig. 7A–C. The functional analysis results indicated the essential roles of OSBPL3 in regulatory network signaling.

4. Discussion

The oxysterol-binding protein (OSBP) and OSBP-related protein (ORP) family consist of various proteins with highly-related gene

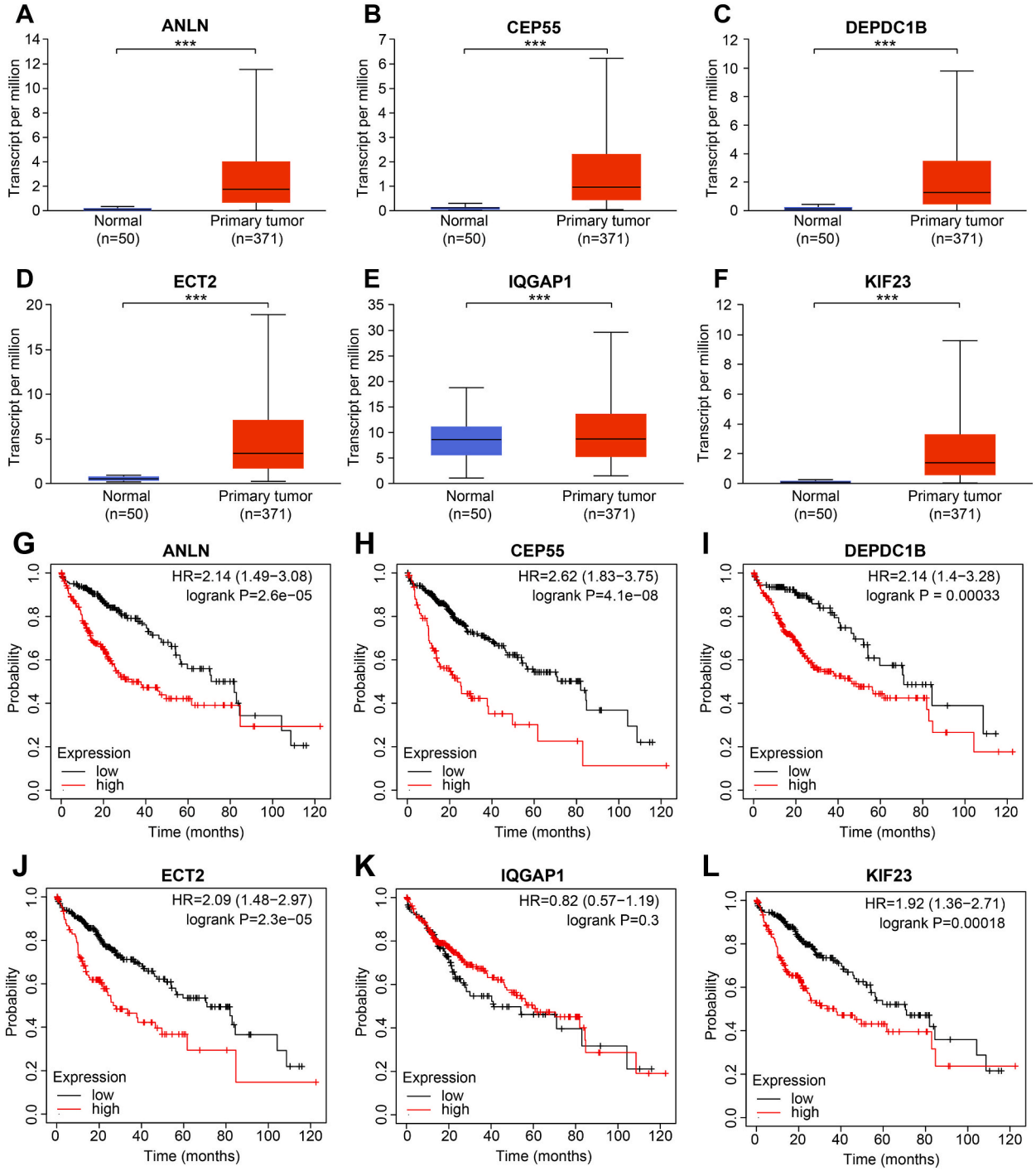

Fig. 6. Upregulated expression of all hub genes indicates the poor survival of patients with LIHC. (A–F) Transcription levels of six hub genes in the LIHC cohort. (G–L) Kaplan-Meier survival curves indicate that patients with LIHC with high OSBPL3 expression have shorter OS. Abbreviations: LIHC, liver hepatocellular carcinoma; OS, overall survival.

sequences. Typical OSBPs contain two major functional structures, including a highly-conserved OSBP-related domain at the carbon terminal and a pleckstrin homology domain at the nitrogen terminal [23,24]. Accumulating evidence have shown that OSBPs played an essential role in regulating lipid metabolism, vesicular transport, and heterogeneous membrane lipid distribution [25,26]. The disruption of lipid distribution or aberrant metabolism caniinduce various diseases including neurodegenerative disease, metabolic dysregulation, and cancers [27].

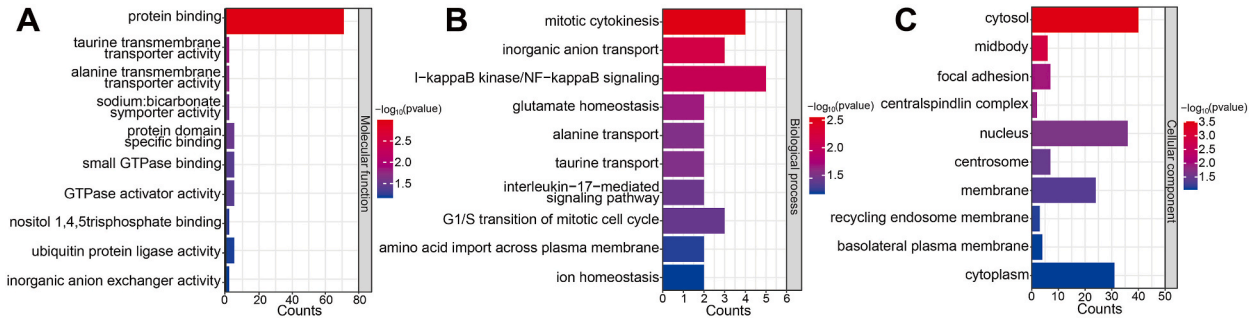

Fig. 7. Gene set enrichment analysis based on OSBPL3-related DEGs. (A–C) Gene ontology functional enrichment analysis results of the top 30 enriched pathways of three major categories, namely biological processes, cellular components, and molecular functions, respectively. Abbreviations: OSBPL3, oxysterol-binding protein-like 3; DEGs, differentially expressed genes.

Not surprisingly, the dysregulated levels of OSBPs have been observed in various cancers, indicating that OSBPs might be pivotal drivers for oncogenesis and tumor progression [28,29]. Whether the involvement of OSBPs in cancers depends upon their signaling conduction or lipid transfer functions needs further characterization. Recent studies showed that ORP4 expression was elevated in cancer cells and exerted an auxo-action effect on cancer cell proliferation and survival [30,31], which was considered as a potential biomarker for a poor prognosis [32]. Moreover, highly expressed ORP5 increased the invasion rate of tumor cells and was positively associated with poor prognosis, especially in metastasis-positive patients [33].

OSBPL3, located at chromosome 7p15.3, has emerged to play critical roles in human cancers through modulating diverse cellular functions. In the past few decades, the abnormal upregulation of OSBPL3 has been uncovered in various malignancies, including colorectal adenocarcinoma, osteosarcoma, testicular cancer, and lymphoma [12,34–36], indicating the oncogenic roles of OSBPL3. However, the roles of OSBPL3 in tumor inhibition has also been reported in lymphoma [37]. In our study, the comprehensive expression signature of OSBPL3 was investigated by a pan-cancer analysis with attention to the LIHC cohort. Consistent with previous findings, we discovered that OSBPL3 was significantly upregulated in most types of human cancers. Moreover, we indicated the promising clinical significance of OSBPL3 by showing its relationship with the clinicopathological characteristics of patients with LIHC, such as advanced tumor stages and poor outcomes. Similar to our results, Zhang et al. found that the expression levels of OBSPL3 were critically higher in CRC tumor tissues than in normal controls, and overexpressed OSBPL3 was positively correlated with shortened survival and low CRC differentiation [13]. Additionally, OSBPL3 expression could be a favorable indicator for the better stratification of clinical outcomes of patients with CRC [14]. Researchers have proposed that OSBPL3 might function as a promoter of cancer cell proliferation, invasion, and migration. Moreover, hyperphosphorylated OSBPL3 selectively interacted with the membrane protein vesicle-associated membrane protein-associated protein A (VAPA) of the endoplasmic reticulum, resulting in the stimulation of *R*-Ras signaling. The ORP3–VAPA interaction boosted the downstream AktS473 signaling pathway and β1-integrin activity, modulating the adhesion characteristic and cell signaling conduction to foster cancer cell malignancy [10,38]. Chou et al. found that OSBPL3 was an important driver for stimulating the *R*-Ras/Akt pathway, serving as a promising therapeutic target in gastric cancer [39].

Recently, significant developments have been made in cancer immunology, bringing about novel immunotherapy strategies for LIHC. Exploring the interaction between oncogenesis and the host immune system is important for discovering available effective prognostic biomarkers and therapeutic targets [40,41]. Previous studies have shown that a tumor immune microenvironment is shaped by immune infiltration status to a large extent [42,43]. In our study, we revealed the correlation between OSBPL3 expression and immune-cell infiltration status and immune purity in LIHC, providing novel insights into LIHC immunotherapy.

Disease phenotypes depend on a complex network of functional synergy between multiple biomolecules [44,45], among which PPIs are critical regarding multifunctionality, specificity, and applicability. Developing computational models for analyzing massive datasets has been a crucial approach for broadening our understanding of diverse phenotypic disorders, including human cancers [44]. In our study, we performed a computational analysis on the integrated informative data to gain novel insights into LIHC. A total of six hub genes were identified based on the OSBPL3-related PPI network (*ANLN*, *CEP55*, *DEPDC1B*, *ECT2*, *IQGAP1*, and *KIF23*). Intriguingly, the transcription levels of all six hub genes increased significantly in the LIHC cohort, implying their clinical significance in its prognosis. Anillin (ANLN) was found to be upregulated in various cancers, including LIHC, and overexpressed ANLN was critically correlated with a poor prognosis in patients with cancer [46]. Moreover, a recent study showed that ANLN promoted tumor cell growth in hepatitis B virus-related LIHC [47]. Yang et al. showed that CEP55 played an oncogenic role in LIHC via the PI3k/Akt pathway [48]. Collectively, these six hub genes might be high-risk factors for LIHC and might significantly affect hepatocarcinogenesis. Our findings provide novel insights into LIHC occurrence and development and further investigation of underlying mechanisms is necessary.

5. Conclusions

OSBPL3 transcription level was critically upregulated in the LIHC and there existed a close correlation between overexpressed OSBPL3 and the clinical features especially poor outcomes of patients with LIHC. We also revealed the fundamental roles of OSBPL3 in LIHC by constructing the comprehensive biological network, broadening our understanding of LIHC initiation and progression.

Collectively, our findings provided new perspectives for monitoring and intervening LIHC by targeting OSBPL3.

Data sharing statement

All data generated or analyzed presented in this study are included in this article [and its supplementary information files]. The datasets used and/or analyzed during the current study available from the corresponding author on reasonable request.

Author contributions

Lanjuan Li conceived and designed the experiments.
Yuanshuai Su and Chen Xue performed the experiments and analyzed and interpreted the data.
Xinyu Gu, Yu Sun and Renfang Zhang contributed reagents, materials, analysis tools and wrote the paper.
All authors read and approved the final manuscript.

Declaration of competing interest

The authors declare that they have no known competing financial interests or personal relationships that could have appeared to influence the work reported in this paper.

Acknowledgments

This work was supported by the National Key Research and Development Program of China (81790631) and the Independent Task of State Key Laboratory for Diagnosis and Treatment of Infectious Diseases (2022zz10).

References

[1] D. Anwanwan, et al., Challenges in liver cancer and possible treatment approaches, Biochim. Biophys. Acta Rev. Canc 1873 (1) (2020), 188314, https://doi.org/10.1016/j.bbcan.2019.188314.
[2] H. Sung, et al., Global cancer statistics 2020: GLOBOCAN estimates of incidence and mortality worldwide for 36 cancers in 185 countries, CA Cancer J. Clin. 71 (3) (2021) 209–249, https://doi.org/10.3322/caac.21660.
[3] C. Li, et al., Analysis of clinicopathological characteristics and prognosis of young patients with hepatocellular carcinoma after hepatectomy, J. Clin. Transl. Hepatol. 8 (3) (2020) 285–291, https://doi.org/10.14218/jcth.2020.00021.
[4] F. Bray, et al., Global cancer statistics 2018: GLOBOCAN estimates of incidence and mortality worldwide for 36 cancers in 185 countries, CA Cancer J. Clin. 68 (6) (2018) 394–424, https://doi.org/10.3322/caac.21492.
[5] L. Kulik, et al., Epidemiology and management of hepatocellular carcinoma, Gastroenterology 156 (2) (2019) 477–491, https://doi.org/10.1053/j.gastro.2018.08.065.
[6] C.C. Gregorio-King, et al., ORP-3, a human oxysterol-binding protein gene differentially expressed in hematopoietic cells, Blood 98 (7) (2001) 2279–2281, https://doi.org/10.1182/blood.v98.7.2279.
[7] M. Lehto, et al., Targeting of OSBP-related protein 3 (ORP3) to endoplasmic reticulum and plasma membrane is controlled by multiple determinants, Exp. Cell Res. 310 (2) (2005) 445–462, https://doi.org/10.1016/j.yexcr.2005.08.003.
[8] M. Weber-Boyvat, et al., Oxysterol-binding proteins: functions in cell regulation beyond lipid metabolism, Biochem. Pharmacol. 86 (1) (2013) 89–95, https://doi.org/10.1016/j.bcp.2013.02.016.
[9] D. Yan, et al., Oxysterol binding protein induces upregulation of SREBP-1c and enhances hepatic lipogenesis, Arterioscler. Thromb. Vasc. Biol. 27 (5) (2007) 1108–1114, https://doi.org/10.1161/atvbaha.106.138545.
[10] M. Lehto, et al., The R-Ras interaction partner ORP3 regulates cell adhesion, J. Cell Sci. 121 (Pt 5) (2008) 695–705, https://doi.org/10.1242/jcs.016964.
[11] I. Gashaw, et al., Gene signatures of testicular seminoma with emphasis on expression of ets variant gene 4, Cell. Mol. Life Sci. 62 (19–20) (2005) 2359–2368, https://doi.org/10.1007/s00018-005-5250-9.
[12] D. Juric, et al., Gene expression profiling differentiates germ cell tumors from other cancers and defines subtype-specific signatures, Proc. Natl. Acad. Sci. U. S. A. 102 (49) (2005) 17763–17768, https://doi.org/10.1073/pnas.0509082102.
[13] M. Zhang, et al., The relationships of OSBPL3 expression with KI-67 expression and KRAS mutations in CRC: implications for diagnosis and prognosis, BMC Med. Genom. 15 (1) (2022) 259, https://doi.org/10.1186/s12920-022-01402-w.
[14] P. Xu, et al., Downregulation of ORP3 correlates with reduced survival of colon cancer patients with advanced nodal metastasis and of female patients with grade 3 colon cancer, Int. J. Mol. Sci. 21 (16) (2020), https://doi.org/10.3390/ijms21165894.
[15] D.S. Chandrashekar, et al., UALCAN: an update to the integrated cancer data analysis platform, Neoplasia 25 (2022) 18–27, https://doi.org/10.1016/j.neo.2022.01.001.
[16] A. Lánczky, et al., Web-based survival analysis tool tailored for medical Research (KMplot): development and implementation, J. Med. Internet Res. 23 (7) (2021), e27633, https://doi.org/10.2196/27633.
[17] E. Cerami, et al., The cBio cancer genomics portal: an open platform for exploring multidimensional cancer genomics data, Cancer Discov. 2 (5) (2012) 401–404, https://doi.org/10.1158/2159-8290.Cd-12-0095.
[18] S.V. Vasaikar, et al., LinkedOmics: analyzing multi-omics data within and across 32 cancer types, Nucleic Acids Res. 46 (D1) (2018) D956–d963, https://doi.org/10.1093/nar/gkx1090.
[19] D. Szklarczyk, et al., STRING v11: protein-protein association networks with increased coverage, supporting functional discovery in genome-wide experimental datasets, Nucleic Acids Res. 47 (D1) (2019) D607–d613, https://doi.org/10.1093/nar/gky1131.
[20] N.T. Doncheva, et al., Cytoscape StringApp: network analysis and visualization of proteomics data, J. Proteome Res. 18 (2) (2019) 623–632, https://doi.org/10.1021/acs.jproteome.8b00702.
[21] B.T. Sherman, et al., DAVID: a web server for functional enrichment analysis and functional annotation of gene lists (2021 update), Nucleic Acids Res. 50 (W1) (2022) W216–W221, https://doi.org/10.1093/nar/gkac194.
[22] T. Li, et al., TIMER: a web server for comprehensive analysis of tumor-infiltrating immune cells, Cancer Res. 77 (21) (2017) e108–e110, https://doi.org/10.1158/0008-5472.Can-17-0307.
[23] M. Lehto, et al., The OSBP-related protein family in humans, J. Lipid Res. 42 (8) (2001) 1203–1213.

[24] C.J. Jaworski, et al., A family of 12 human genes containing oxysterol-binding domains, Genomics 78 (3) (2001) 185–196, https://doi.org/10.1006/geno.2001.6663.
[25] A. Arora, et al., Coordination of inter-organelle communication and lipid fluxes by OSBP-related proteins, Prog. Lipid Res. 86 (2022), 101146, https://doi.org/10.1016/j.plipres.2022.101146.
[26] V.M. Olkkonen, et al., The OSBP-related proteins (ORPs): global sterol sensors for co-ordination of cellular lipid metabolism, membrane trafficking and signalling processes? Biochem. Soc. Trans. 34 (Pt 3) (2006) 389–391, https://doi.org/10.1042/bst0340389.
[27] M.T. Snaebjornsson, et al., Greasing the wheels of the cancer machine: the role of lipid metabolism in cancer, Cell Metabol. 31 (1) (2020) 62–76, https://doi.org/10.1016/j.cmet.2019.11.010.
[28] X. Du, et al., The role of oxysterol-binding protein and its related proteins in cancer, Semin. Cell Dev. Biol. 81 (2018) 149–153, https://doi.org/10.1016/j.semcdb.2017.07.017.
[29] L. Song, et al., ORP5 promotes tumor metastasis via stabilizing c-Met in renal cell carcinoma, Cell Death Dis. 8 (1) (2022) 219, https://doi.org/10.1038/s41420-022-01023-3.
[30] M. Charman, et al., Oxysterol-binding protein (OSBP)-related protein 4 (ORP4) is essential for cell proliferation and survival, J. Biol. Chem. 289 (22) (2014) 15705–15717, https://doi.org/10.1074/jbc.M114.571216.
[31] W. Zhong, et al., ORP4L is essential for T-cell acute lymphoblastic leukemia cell survival, Nat. Commun. 7 (2016), 12702, https://doi.org/10.1038/ncomms12702.
[32] G. Pan, et al., OSBP-related protein 4L promotes phospholipase Cβ3 translocation from the nucleus to the plasma membrane in Jurkat T-cells, J. Biol. Chem. 293 (45) (2018) 17430–17441, https://doi.org/10.1074/jbc.RA118.005437.
[33] Y. Koga, et al., Oxysterol binding protein-related protein-5 is related to invasion and poor prognosis in pancreatic cancer, Cancer Sci. 99 (12) (2008) 2387–2394, https://doi.org/10.1111/j.1349-7006.2008.00987.x.
[34] D. Tsafrir, et al., Relationship of gene expression and chromosomal abnormalities in colorectal cancer, Cancer Res. 66 (4) (2006) 2129–2137, https://doi.org/10.1158/0008-5472.Can-05-2569.
[35] T. Ozaki, et al., Chromosomal alterations in osteosarcoma cell lines revealed by comparative genomic hybridization and multicolor karyotyping, Cancer Genet. Cytogenet. 140 (2) (2003) 145–152, https://doi.org/10.1016/s0165-4608(02)00685-4.
[36] M. Lehto, et al., Subfamily III of mammalian oxysterol-binding protein (OSBP) homologues: the expression and intracellular localization of ORP3, ORP6, and ORP7, Cell Tissue Res. 315 (1) (2004) 39–57, https://doi.org/10.1007/s00441-003-0817-y.
[37] S.N. Njeru, et al., Aneuploidy-inducing gene knockdowns overlap with cancer mutations and identify Orp3 as a B-cell lymphoma suppressor, Oncogene 39 (7) (2020) 1445–1465, https://doi.org/10.1038/s41388-019-1073-2.
[38] M. Weber-Boyvat, et al., OSBP-related protein 3 (ORP3) coupling with VAMP-associated protein A regulates R-Ras activity, Exp. Cell Res. 331 (2) (2015) 278–291, https://doi.org/10.1016/j.yexcr.2014.10.019.
[39] Q. Hu, et al., Oxysterol binding protein-like 3 (OSBPL3) is a novel driver gene that promotes tumor growth in part through R-Ras/Akt signaling in gastric cancer, Sci. Rep. 11 (1) (2021), 19178, https://doi.org/10.1038/s41598-021-98485-9.
[40] J.M. Llovet, et al., Immunotherapies for hepatocellular carcinoma, Nat. Rev. Clin. Oncol. 19 (3) (2022) 151–172, https://doi.org/10.1038/s41571-021-00573-2.
[41] B. Ruf, et al., Immunobiology and immunotherapy of HCC: spotlight on innate and innate-like immune cells, Cell. Mol. Immunol. 18 (1) (2021) 112–127, https://doi.org/10.1038/s41423-020-00572-w.
[42] Y. Wu, et al., CircLATS2 regulates miR-520a-3p/E2F7/p-VEGFR2 signaling pathway to promote hepatocellular carcinoma progression and angiogenesis, JAMA Oncol. 2022 (2022), 3744560, https://doi.org/10.1155/2022/3744560.
[43] Y. Yang, Cancer immunotherapy: harnessing the immune system to battle cancer, J. Clin. Invest. 125 (9) (2015) 3335–3337, https://doi.org/10.1172/jci83871.
[44] J. Nielsen, Systems biology of metabolism, Annu. Rev. Biochem. 86 (2017) 245–275, https://doi.org/10.1146/annurev-biochem-061516-044757.
[45] P. Xing, et al., A fast approach to detect gene-gene synergy, Sci. Rep. 7 (1) (2017), 16437, https://doi.org/10.1038/s41598-017-16748-w.
[46] Y. Shi, et al., Comprehensive analyses reveal the carcinogenic and immunological roles of ANLN in human cancers, Cancer Cell Int. 22 (1) (2022) 188, https://doi.org/10.1186/s12935-022-02610-1.
[47] Y.F. Lian, et al., Anillin is required for tumor growth and regulated by miR-15a/miR-16-1 in HBV-related hepatocellular carcinoma, Aging (Albany NY) 10 (8) (2018) 1884–1901, https://doi.org/10.18632/aging.101510.
[48] Y.F. Yang, et al., SPAG5 interacts with CEP55 and exerts oncogenic activities via PI3K/AKT pathway in hepatocellular carcinoma, Mol. Cancer 17 (1) (2018) 117, https://doi.org/10.1186/s12943-018-0872-3.